Electronic Supplementary Material (ESI) for ChemComm.

Supplementary Information

Long-cycle Zn-air batteries at high depth of discharge enabled by robust Zn|electrolyte interface

Jinxian Wang, ‡ Danni Deng, ‡ Yuchao Wang, Huanran Zheng, Mengjie Liu,

Yingbi Chen, Yu Bai, Jiabi Jiang, Xinran Zheng, Peiyao Yang, Qiumei Wu,

Xiang Xiong and Yongpeng Lei*

State Key Laboratory of Powder Metallurgy, Central South University,

Changsha 410083, China.

Correspondence and requests for materials should be addressed to Y. Lei.

（lypkd@163.com）

Experimental Section

Material. All chemicals were from commercial sources and used without further purification. Potassium hydroxide (KOH, AR), Methanol (CH_3OH, AR), Zinc acetate dihydrate ($Zn(Ac)_2·2H_2O$, AR), Zinc nitrate hexahydrate ($Zn(NO_3)_2·6H_2O$, 98%) and N,N-Dimethylformamide (DMF, AR) were purchased from Sinopharm Chemical Reagent Co., Ltd, China. 2-Methylimidazole ($C_4H_6N_2$, 98%), Acrylamide (AM, 99%), N,N'-Methylenebis(acrylamide) (MBAA, 99%) and Potassium persulfate ($K_2S_2O_8$, 99.99%) were purchased from Shanghai Aladdin Biochemical Technology Co., Ltd. Acrylic acid (AA, >99%), Iron (III) acetylacetonate ($C_{15}H_{21}FeO_8$, AR), Polytetrafluoroethylene emulsion (PTFE, 60%), Dimethyl sulfoxide (DMSO, AR) and Iridium C electrocatalyst (5 wt%) were purchased from Shanghai Macklin Biochemical Technology Co., Ltd. Sodium borohydride($NaBH_4$, AR) were purchased from Tianjin Kemiou Chemical Reagent Co., Ltd. Commercial Pt/C (20 wt%) electrocatalyst and Nafion solution (5 wt%, D520) were purchased from Shanghai Hesen Electric Co., Ltd. Waterproof breathable membrane and Ni foam were purchased from Changsha spring new energy technology Co., Ltd. N_2 (99.99%) and O_2 (99.99%) were purchased from Changsha Xinxiang Gas Chemical Co., Ltd. Distilled water (18.2 MΩ) was obtain from milli-Q system (UPT).

Synthesis of Fe@NC. It was synthesized via optimized top-down strategy at room temperature (RT). Typically, $Zn(NO_3)_2·6H_2O$ (1.069 g) was dissolved in 10 mL methanol with stirring in flask A. $C_{15}H_{21}FeO_8$ (140 mg) and DMF (2 mL) were dissolved in flask A under ultrasound for 5 min to form a red-brown solution. $C_4H_6N_2$ (1.161 g) was dissolved in 10 mL methanol with stirring in flask B to form a clear solution. Then, flask B was subsequently quickly added into flask A with vigorous stirring for 30 min. After reacting for 24 h at RT, the upper layer was red-brown solution and the lower layer was red-brown precipitate. The obtained product was separated by centrifugation and washed subsequently with DMF and methanol for three times respectively and finally dried at 70 °C under vacuum for 12 h to obtain light yellow precursor powder Fe/ZIF-8. The same process was adopted for the synthesis of white powder ZIF-8 without $C_{15}H_{21}FeO_8$. The prepared powder was heated to 900 ℃ (heating rate of 5 ℃ min^{-1}) under N_2 and maintained for 2 h for pyrolysis. After being naturally cooled to room temperature, the black powder Fe@NC was accordingly obtained without further processing.

Synthesis of Fe@BNC. In a typical process, a certain amount of Fe@NC powder and $NaBH_4$ (the mass ratio of Fe@NC to $NaBH_4$ was 2:1) were first grounded thoroughly for 30 min. The as-prepared powder was heated to 800 ℃ (heating rate of 5 ℃ min^{-1}) under N_2 and maintained for 30 min. The obtained powder was washed with distilled water for several times and finally dried at 70 °C under vacuum for 12 h to

obtain Fe@BNC powder. As a comparison, under the same preparation conditions, further adjusting secondary calcination temperature (600 ℃, 800 ℃ and 1000 ℃, respectively) and the mass ratio of Fe@NC to $NaBH_4$ (1:1, 2:1 and 5:1, respectively). Among them, when the second calcination temperature is 800℃ and the mass ratio of Fe@NC to $NaBH_4$ is 2: 1, the electrocatalytic oxygen reduction reaction (ORR) performance of Fe@BNC is the best.

Synthesis of the PAA-PAM hydrogel electrolyte. The stretchable gel electrolyte was fabricated by a free radical polymerization approach. The function of the initiator is to promote the formation of free radicals and initiate polymerization. Typically, 2 g of AM, 2 g of AA, 9 mL of distilled water and 6 mL of DMSO were mixed under magnetic stirring for 5 min. Then, 10 mg of MBAA (Crosslinking agent) and 25 mg of $K_2S_2O_8$ (Initiator) were added in the above solution. The resultant solution was poured into a transparent box (Length, width and height are 8.5, 8.5, and 2.5 cm, respectively). Then the box was sealed with tape and placed in an oven at 80 °C for 300 min. The as-prepared PAA-PAM hydrogel was immersed in the 6 M KOH + 0.2 M $Zn(Ac)_2 \cdot 6H_2O$ electrolyte for 72 h before use.

Material characterization. The XRD patterns were recorded on an X-ray diffractometer (D/max 2550) with Cu Kα radiation at a scan rate of 10° min^{-1} from 5° to 90°. X-ray photoelectron spectroscopy (XPS) was carried out on a Thermo Scientific ESCALab 250Xi+ XPS instrument using 150W monochromated Al Kα (1486.6 eV). The in situ optical visualization was obtained by M230-HD228S microscope. The three-dimensional confocal laser scanning microscope (3D CLSM) topographic images of Zn anodes were analyzed with a 3D laser microscopic imaging system (VK-150K). Scanning electron microscopy (SEM) images of Zn anode before/after cycling were measured by a Zeiss Gemini Sigma 300 VP SEM.

Electrochemical measurement. The electrochemical tests are carried out in an environmental chamber at RT. All the electrochemical tests were carried out in a conventional three-electrode system on a CHI 660 and CHI 730 electrochemical station (Shanghai Chenhua, China) in 0.1 M KOH. The counter electrode and the reference electrode were a platinum sheet electrode and a saturated calomel electrode (SCE), respectively. The working electrode was a rotating disk electrode (RDE) (Pine Research Instrument, USA) loaded with catalyst ink (Catalyst loading: 0.3 mg cm^{-2}), where the disk electrode was a glassy carbon electrode with a diameter of 5.0 mm. The area of the disk electrode was 0.196 cm^2. All recorded potentials were calibrated to the reversible hydrogen electrode (RHE) according to $E_{(RHE)} = E_{(SCE)} + (0.241 + 0.0591\ pH)$ V.

To prepare the catalyst ink, 6 mg catalysts and 40 μL of Nafion solution were dispersed in 960 μL water-isopropanol solution (volume ratio of 3:1) by sonicating for 1 h to form a homogeneous ink. Then 10 μL of catalyst ink was dropped onto the glass carbon electrode, and dried at 25 °C. The electrocatalysts were loaded

on the working electrode by a drop-casting method. Specifically, 5.0 mg electrocatalyst was firstly dispersed in the mixed solution containing 960 μL isopropanol aqueous solution (isopropanol 240 μL, deionized water 720 μL) and 40 μL Nafion solution (5.0 wt.% in ethanol). The mixed solution was ultrasonicated for 2 h to form a homogenous suspension. Then, 10 μL of the suspension was dropped onto the disk electrode, which was mechanically polished using Al_2O_3 powder and ultrasonically washed by deionized water and ethanol. After the evaporation of the solvent, the working electrode was successfully prepared for further electrochemical evaluations.

The samples were firstly activated in N_2-saturated 0.1 M KOH by cyclic voltammetry (CV) method (scan rate of 100 mV s^{-1}) under -0.6 to 0.1 V vs. SCE to reach a stable condition. When the CV curves completely coincide, the activation process is terminated. Before ORR test, the O_2 was bubbled into electrolyte to maintain O_2 saturation during the ORR process. Linear sweep voltammetry (LSV) curves were recorded in the O_2-saturated 0.1 M KOH ranging from -0.9 to 1 V vs. SCE (a scan rate of 5 mV s^{-1}) at 400-1600 rpm with 100% iR-compensation. The electrochemical impedance spectroscopy (EIS) tests were carried out at -0.2 V vs. SCE. The spectra were recorded in a frequency range from 10^{-2} to 10^5 Hz with a voltage amplitude of 5.0 mV. The accelerated degradation tests were performed by cycling the catalyst between -0.5 and 0 V vs. SCE with a scan rate of 100 mV s^{-1} in O_2-saturated 0.1 M KOH. And stability test was also performed by chronoamperometric at -0.20 V vs. SCE for 30,000 s with the RDE at a rotation rate of 1600 rpm. The methanol crossover effect was explored by chronoamperometric responses at -0.2 V vs. SCE for 1200 s. In this process, 6 mL of 3 mol L^{-1} methanol was injected into the O_2-saturated 0.1 M KOH electrolyte.

The $4e^-$ pathway of catalysts was estimated by the following equations:

$$\frac{1}{j} = \frac{1}{j_L} + \frac{1}{j_k} = \frac{1}{B\omega^{1/2}} + \frac{1}{j_k} \quad (1)$$

$$B = 0.2nFC_0(D_0)^{2/3}\upsilon^{-1/6} \quad (2)$$

$$j_k = nFkC_0 \quad (3)$$

Where j is the measured current density; j_k and j_L represent the kinetic and limiting current densities, respectively; ω is the rotation rate of RDE (rpm), B is determined by the slope of koutechy-Levich (K-L) plot according to Levich equation (3), n represents calculated number of the transferred electron in ORR; F is the Faraday constant (F = 96485 C mol^{-1}); C_0 is the bulk concentration for O_2 (1.2×10^{-6} mol cm^{-3}) dissolved in 0.1M KOH solution; D_0 is the diffusivity of O_2 ($1.9 \times$ 10-5 cm^2 s^{-1}); v is the kinematic viscosity of electrolyte (0.01 cm^2 s^{-1}), and k is the electron-transferred rate constant.

The hydrogen peroxide yield (H_2O_2 %) and the electron transfer number (n) were calculated with the following equations:

$$H_2O_2\,(\%) = 200 \times \frac{\frac{I_r}{N}}{I_d + \frac{I_r}{N}} \quad (4)$$

$$n = 4 \times \frac{I_d}{I_d + \frac{I_r}{N}} \quad (5)$$

Where I_d is the disk current, I_r is the ring current, and N is the current collection efficiency of Pt ring and N=0.37.

For oxygen evolution reaction (OER) measurement, 20 μL of ink was dropped onto the carbon paper (effective area of 0.25 cm^2) and dried at 25 °C for 0.5 h. The OER electrochemical tests were performed in 1.0 mol L^{-1} KOH solution. Before test, the samples were firstly activated by CV method under 0-0.8 V vs. SCE (scan rate of 100 mV s^{-1}) to reach a stable condition. When the CV curves completely coincide, the activation process is terminated. LSV curves were obtained at a scan rate of 5 mV s^{-1} from 0 to 0.8 V vs. SCE with 100% iR-compensation. Stability test was performed by chronoamperometric at 0.52 V vs. SCE for 20,000 s. The EIS tests were carried out at 0.52 V vs. SCE. The spectra were recorded in a frequency range from 10^{-2} to 10^5 Hz with a voltage amplitude of 5.0 mV. $E_{1/2}$ (half-wave potential, the potential to reach half of the limiting current density) and E_{10} (potential at the current density of 10 mA cm^{-2}) served as the index to reveal the ORR and OER activity, respectively. The bifunctional performance (ΔE) was the potential gap between $E_{1/2}$ and E_{10}.

Tafel slopes were calculated based on the data of the LSV profiles according to Tafel equation: $\eta = b\log(j/j_0)$, where η is the overpotential ($\eta = |E_{(RHE)}\text{-}1.23\ V|$), b is the Tafel slope, j is the recorded disk current density, and j_0 is the exchange current density.

Solid-state Zn-air batteries (SS ZABs) measurement. The SS ZABs were fabricated in a sandwich structure. Particularly, a polished zinc foil (0.5 mm thickness), the catalysts coated carbon cloth (0.25 mg cm^{-2}) and a PAA-PAM gel were used as anode, air electrode and solid electrolyte, respectively. Besides, using "Pt/C+Ir/C" material as a reference. And the specfic preparation process is that commercial Pt/C (20 wt%) and Ir/C (5 wt%) are fully physically mixed in the mass ratio of 1: 1 to obtain "Pt/C+Ir/C" materials. The air electrode (cathode) was prepared as follows: the as-prepared catalysts (60 mg), carbon black (10 mg) and PTFE concentrated solution (10 μL) were added to ethanol, then grind until the ethanol volatilizes for 15 min.

Then, it was made into air electrode materials with an area of 1 cm^2. Finally, cathode and anode were placed on the two sides of PAA-PAM gel and fixed with a battery clamp. The battery experiments are carried out at RT. The open-circuit voltage and charge-discharge curve were obtained in a three-electrode configuration using a CHI660E electrochemical workstation. The rate curve, constant current discharge and charge-discharge cycle were performed in the NEWARE battery testing system.

The capacity (C, mAh cm^{-2}) of ZABs was calculated from discharge curves according to the equation:

$$C = I \times t \qquad (6)$$

Where I denotes the discharge current density (mA cm^{-2}), t is the discharge time (h).

The discharge capacity (mAh cm^{-2}) per cycle was calculated from constant current discharge and charge-discharge cycle curves according to the equation:

$$The\ discharge\ capacity\ per\ cycle = i \times t_1 \qquad (7)$$

Where i denotes the current density per cycle (mA cm^{-2}), t_1 is the discharge time per cycle (h).

The power density (P, mW cm^{-2}) of ZABs was calculated based on the equation

$$P = U \times I \qquad (8)$$

Where I is the discharge current density (mA) and U denotes the corresponding voltage (V).

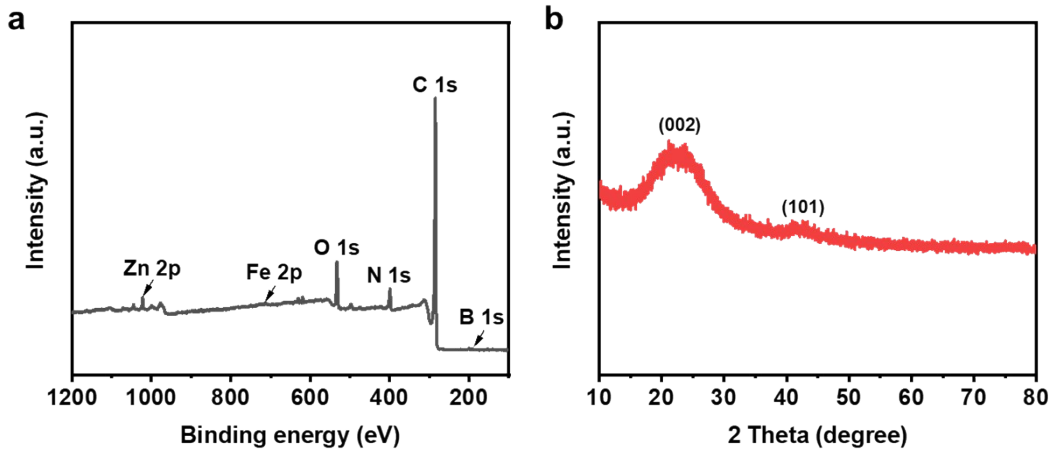

Fig. S1 (a) XPS survey spectra and (b) XRD results of Fe@BNC.

As shown in Fig. S1b, there are two broad peaks at around 24° and 25°, which are attributed to (002) and (100) planes of graphitic carbon, respectively.

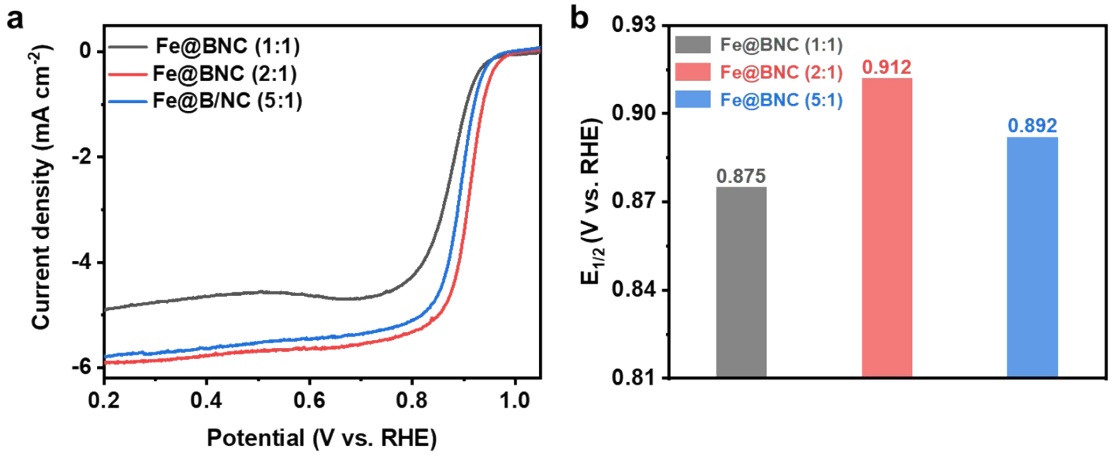

Fig. S2 (a) LSV curves and (b) comparison of $E_{1/2}$ of Fe@BNC obtained by doping different B element contents. Fe@BNC (1:1) means that it was obtained at 800℃ and $m_{Fe@NC}$: m_{NaBH4}=1:1, and so on.

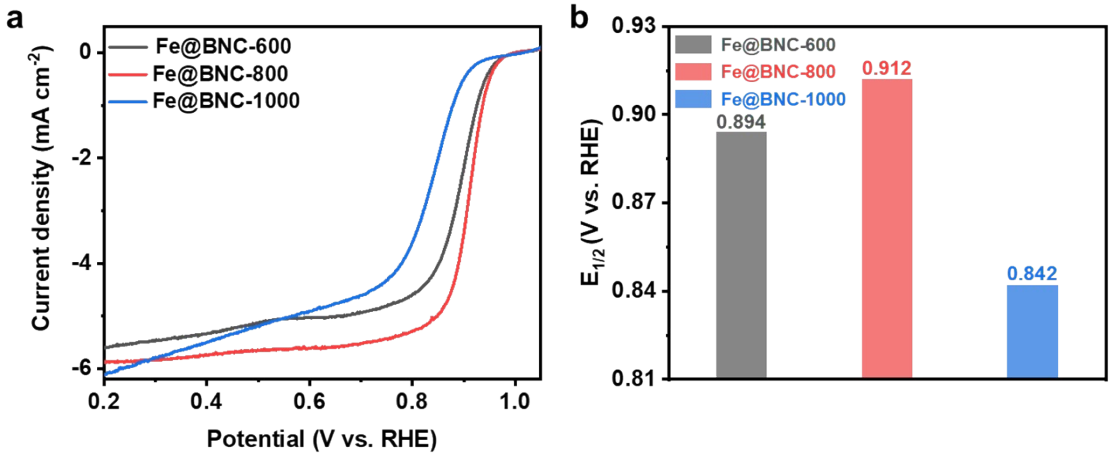

Fig. S3 (a) LSV curves and (b) comparison of $E_{1/2}$ of Fe@BNC obtained at different calcination temperatures. Fe@BNC-600 means that when $m_{Fe@NC}$: m_{NaBH4}=2:1, it was obtained by second calcination at 600℃, and so on.

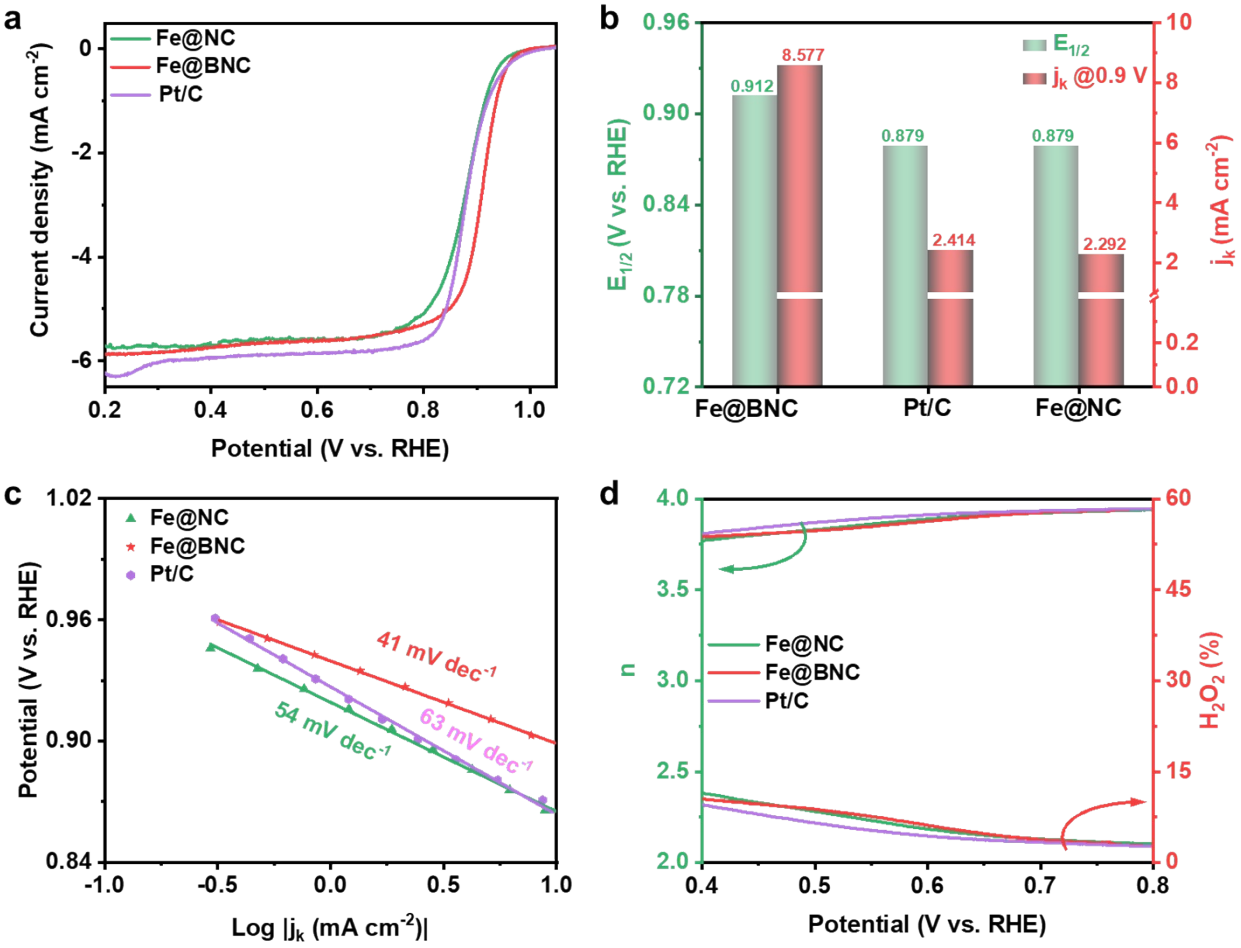

Fig. S4 (a) The LSV curves of Fe@BNC and contrast samples for the ORR. (b) Comparison of $E_{1/2}$ and j_k at 0.9 V vs. RHE for different catalysts. (c) Tafel plots. (d) Electron transfer numbers and H_2O_2 yield of Fe@B/NC, Fe@NC and Pt/C.

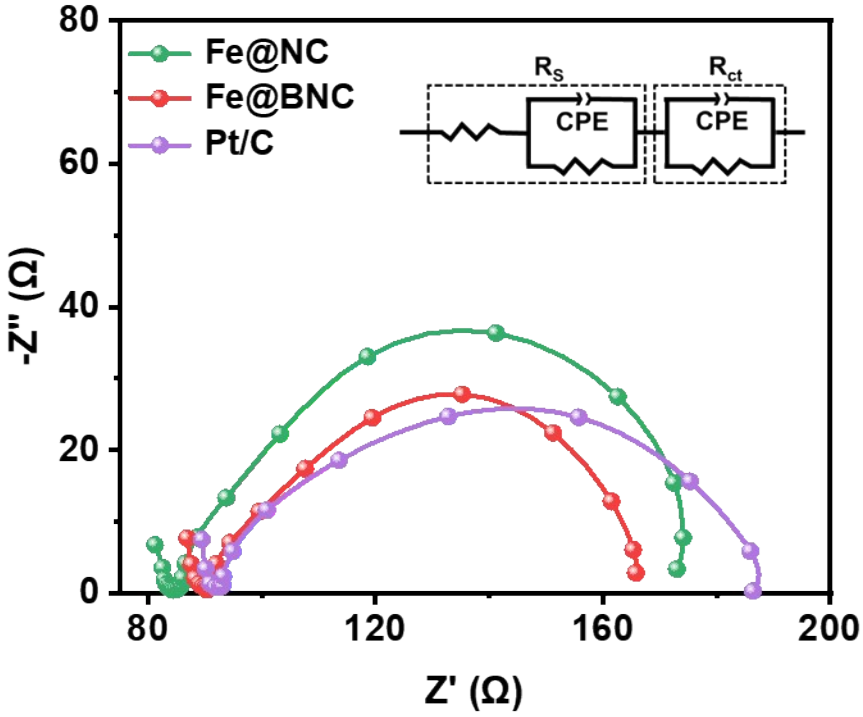

Fig. S5 EIS results of Fe@BNC and contrast samples obtained at 0.81 V. The inset is the fitting circuit. R_s: Solution resistance, R_{ct}: Charge transfer resistance, CPE: Constant phase element.

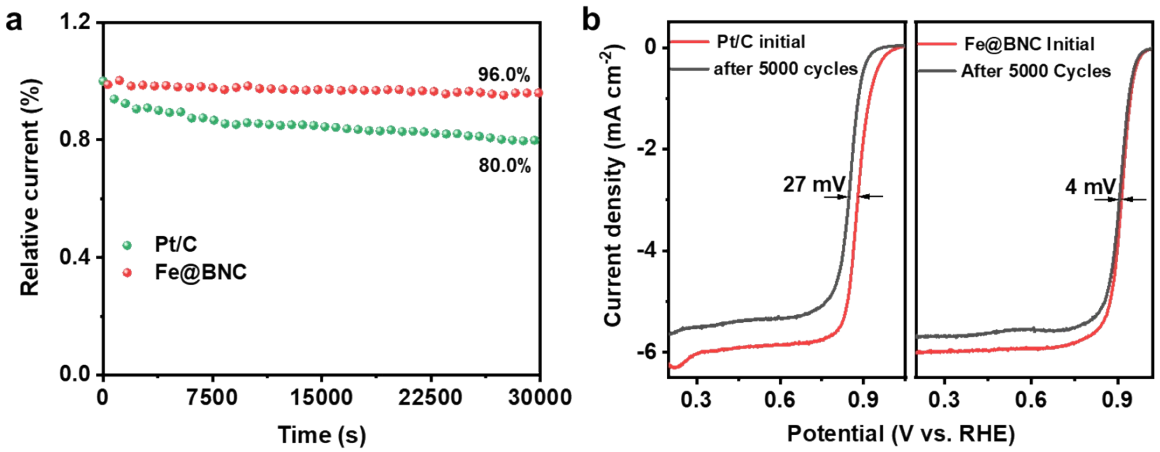

Fig. S6 (a) Relative current-time curves for the ORR of Fe@BNC and Pt/C in 0.1 M KOH. (b) ORR polarization curves of Fe@BNC, Pt/C before and after 5000 potential cycles.

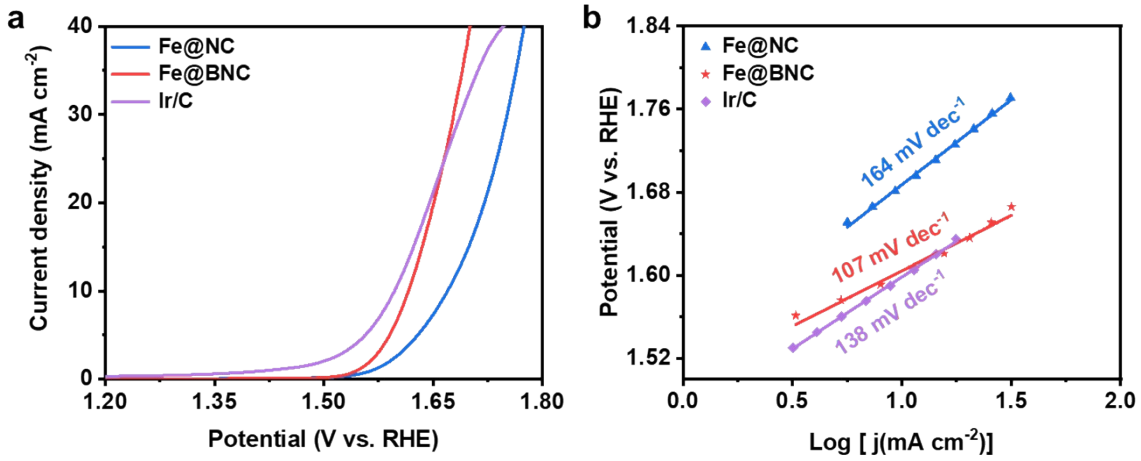

Fig. S7 (a) The LSV curves of Fe@BNC and contrast samples for the OER. (b) Tafel plots.

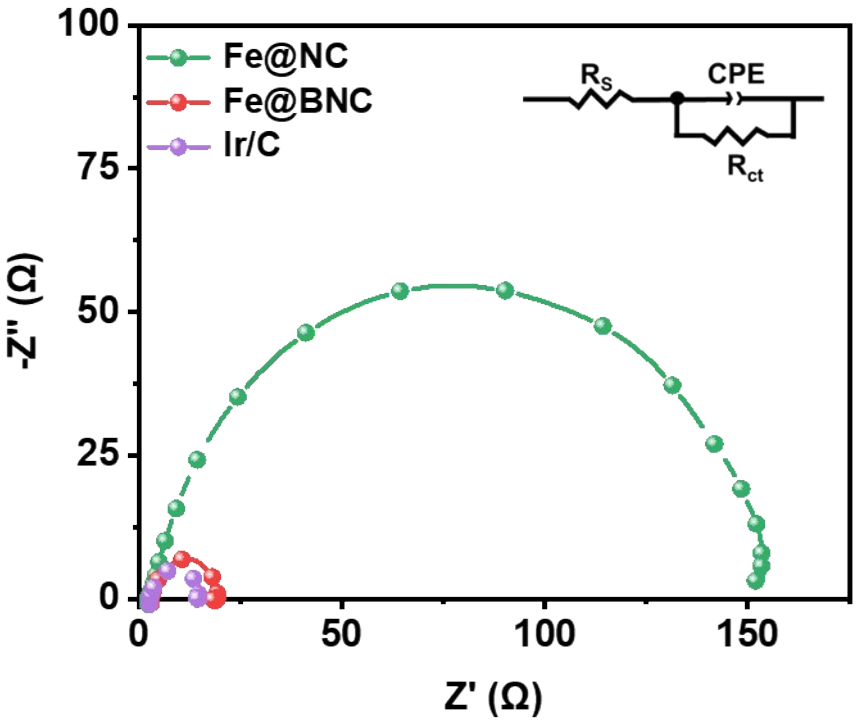

Fig. S8 EIS results of Fe@BNC and contrast samples. The inset is the fitting circuit.

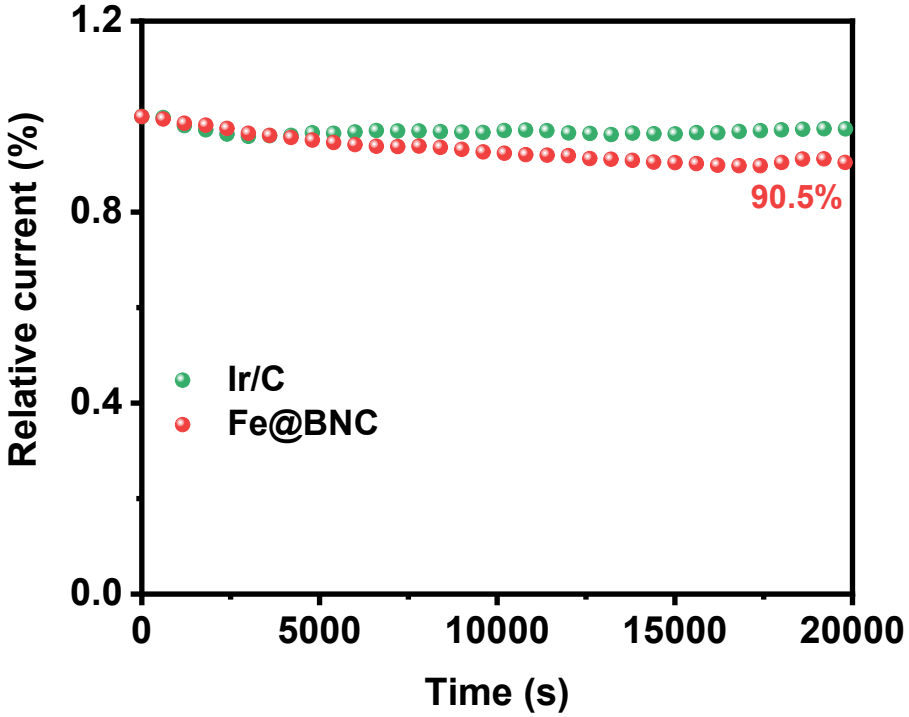

Fig. S9 Relative current-time curves for the OER of Fe@BNC and Ir/C in 1 M KOH.

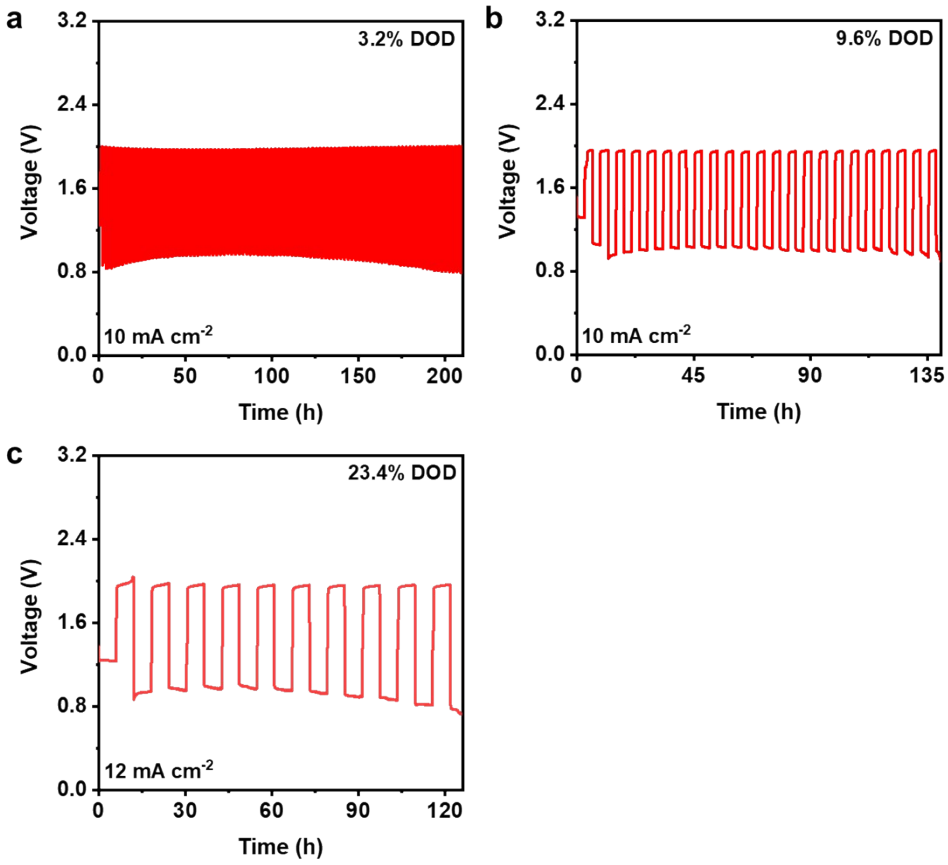

Fig. S10 Galvanostatic cycling curves of ZABs-Fe@BNC at (a) 3.2%, (b) 9.6% and (c) 23.4% DOD per cycle, respectively.

Fig. S10 shows that the ZABs-Fe@BNC at 9.6% DOD exhibits the cycle life of～140 h, which is obviously longer than that at 23.4% DOD but shorter than that at 3.2% DOD. These results strongly prove that the cycle life of solid-state ZABs decreases with the increase of DOD.

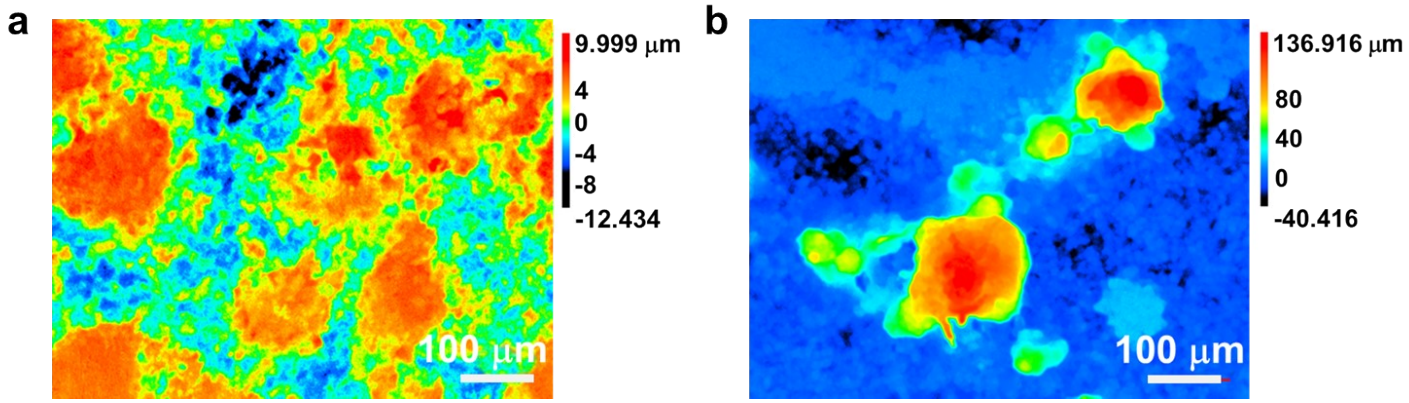

Fig. S11 2D topographic images of Zn plates surface after 36 h of cycling at (a) 3.2% and (b) 23.4% DOD were obtained by a 3D CLSM.

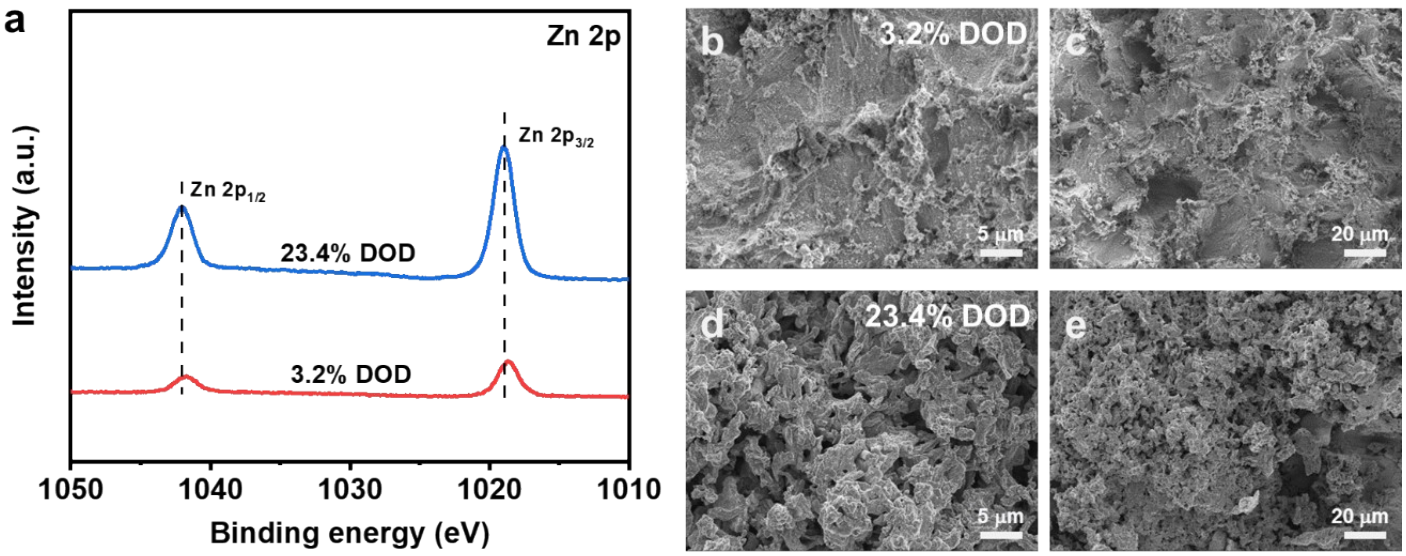

Fig. S12 (a) Zn 2p spectrum of Zn plates after 36 h of cycling. SEM images of Zn plates after 36 h of cycling at (b, c) 3.2% DOD and (d, e) 23.4% DOD, respectively.

The Zn 2p spectrum shows two peaks located at around 1042.1 eV and 1019.0 eV, indexes to Zn $2p_{1/2}$ and Zn $2p_{2/3}$ signals, which indicates the existence of Zn(II) species. The XPS results show that there are ZnO/$Zn(OH)_2$ species on the surface of Zn plates after cycling at different DOD and the consumption of Zn is more at high DOD (Fig. S12a). Scanning electron microscopy (SEM) was further performed. As shown in Fig. S12b, the Zn dendrites are observed on the surface of Zn plates after cycling, and the surface of Zn plates after cycling at 23.4% DOD is rougher than that at 3.2% DOD. (The relevant sentences were added to the revised Supplementary Information, which were marked in yellow.)

Table S1 Performance comparison of reported ZABs at room temperature.

Hydrogel electrolytes	Charge/discharge time per cycle	Discharge capacity per cycle (mAh cm^{-2})	Cycle time (h)@ current density (mA cm^{-2})	Refs.
PAA-PAM	1h/1h 6 h/6 h	10 72	210@10 120@12	This work
P(AA-co-AMPS)/LAP	5 min/5 min	1.67	~146@20	*ACS Nano* **2023**, *17*, 9565.
SSHPE	30 min/30 min	0.5	300@1	*Angew. Chem. Int. Ed.* **2023**, *62*, e202302640.
p18@PAA	10 min/10 min	0.17	40@2	*Adv. Funct. Mater.* **2023**, *33*, 2303719.
PAM	5 min/5 min	1.67	280@20	*Adv. Funct. Mater.* **2023**, *33*, 2300815.
PAAm-co-PVA + PAA-co-PVA	8 h/8 h	8	200@1	*Energy Storage Mater.* **2023**, *59*, 102791.
PAM-SC	3 min/3 min	0.04	42@0.5	*Angew. Chem. Int. Ed.* **2023**, *62*, e202301114.
Starch-PAA (SSHPE)	30 min/30 min	0.5	300@1	*Angew. Chem. Int. Ed.* **2023**, *62*, e202302640
PAM organohydrogel	5 min/5 min	1.67	200@20	*Angew. Chem. Int. Ed.* **2023**, *62*, e202219191.
PAM	5 min/5 min	4.17	100@50	*Nat. Commun.*, **2022**, *13*, 3689.
PAM/MMT organic hydrogel	10 min/10 min	0.33	80@2	*Angew Chem. Int. Ed.* **2022**, *61*, e202115219.
WIS-PAA/CNF	10 min/10 min	0.017	1300@0.1	*Adv. Funct. Mater.* **2022**, *32*, 2203204.
Starch gel-KOH	5 min/5 min	0.17	36@2	*Cell Rep. Phys. Sci.* **2022**, *3*, 100687.
MC/PAM-PDMC	10 min/10 min	0.33	340@2	*Adv. Mater.* **2022**, *34*, 2110585.
PAM-CNF/KOH/KI	10 min/10 min	0.33	75@2	*Energy Storage Mater.* **2021**, *42*, 88.
A-PAA	3 min/3 min	0.1	92@2	*Energy Environ. Sci.* **2021**, *14*, 4926.
G-CyBA/PAAm	5 min/5 min	0.17	100@2	*Energy Environ. Sci.*

				2021, *14*, 4451.
PAMC	5 min/ 5 min	0.42	32@5	*Chem. Eng. J.* **2021**, *417*, 129179.
PAMPS-K/MC	10 min/10 min	0.17	24@1	*ACS Appl. Mater. Interfaces* **2020**, *12*, 11778.
PAM/PAA	3 min/3 min	0.05	10@1	*ACS Sustainable Chem. Eng.* **2020**, *8*, 11501.
PVA	5 min/5 min	0.52	15@6.25	*Adv. Mater.* **2019**, *31*, 1808267.
PANa	5 min/5 min	0.17	160@2	*Adv. Energy Mater.* **2018**, *8*, 1802288.